Experimental and computational study of neutral xenon halides (XeX) in the gas phase for X=F, Cl, Br, and I

Detlef Schröder, Jeremy N. Harvey, Massimiliano Aschi, and Helmut Schwarz
Institut für Organische Chemie, Strasse des 17. Juni 135, D-10623 Berlin, Germany

We report a combined experimental and theoretical study of the xenon monohalide radicals XeX[•] (X=F, Cl, Br, and I) together with their cationic and anionic counterparts XeX[+] and XeX[−]. In brief, the XeX[+] cations are characterized by reasonably strong chemical bonds with significant charge-transfer stabilization, except for X=F. In contrast, the neutral XeX[•] radicals as well as the XeX[−] anions can mostly be described in terms of van der Waals complexes and exhibit bond strengths of only a few tenths of an electron volt. For both XeX[•] and XeX[−] the fluorides (X=F) are the most strongly bound among the xenon halides due to significant covalency in the neutral radical, and to the large charge density on fluoride in the XeX[−] anion, respectively. Mass spectrometric experiments reveal the different behavior of xenon fluoride as compared to the other halides, and in kiloelectron-volt collisions sequential electron transfer according to XeX[+]→XeX[•]→XeX[−] can be achieved allowing one to generate neutral XeX[•] radicals with lifetimes of at least a few microseconds for X=F and I. © *1998 American Institute of Physics.* [S0021-9606(98)02220-X]

I. INTRODUCTION

Since the first rare-gas halide excimer laser was reported in 1975,[1] diatomic xenon halides have been the subject of extensive experimental and theoretical studies. In addition, these species are also of fundamental interest as possible examples of neutral xenon compounds in the +I oxidation state.[2,3] Early computational studies of Hay and Dunning[4] suggested that only the potential curves of the *ionic* $2\,^2\Sigma^+$ and $2\,^2\Pi$ excited states, corresponding to the charge transfer complexes $Xe^{+\bullet}\,X^-$, which are responsible for the laser activity, had a bound minimum; whereas the lower-lying $1\,^2\Sigma^+$ and $1\,^2\Pi$ states were found to be repulsive. This result was, however, in contradiction with detailed experimental studies of the UV emissions occurring upon transitions between the above cited ionic and covalent states.[5,6] These, together with molecular beam scattering experiments[7] have instead demonstrated the existence of attractive potentials in the ground states XeX[•] ($^2\Sigma^+$). These interactions were described in terms of van der Waals forces in all the xenon halides, with the exception of XeF for which the experimental bond length (r_{Xe-F}) of 2.29 Å and a dissociation energy (D_e) of 3.36 kcal/mol were interpreted in terms of a partial covalent character in the ground state.[5,7] Therefore, the xenon monohalides are still of considerable interest,[8] and in particular, the theoretical[9] and experimental characterization of the ground states is still incomplete.

In the present study, the four neutral xenon monohalides as well as the corresponding cations[10] and anions,[11] i.e., XeX[+/°/−] (X=F, Cl, Br, I), have been investigated using a combination of experimental and theoretical approaches. The experiments were performed using neutralization-reionization mass spectrometry (NRMS) whose ability to provide information about the structures and the stability of gaseous neutral species has been widely documented.[12] Thus, collisional neutralization of xenon-halide cations may be affordable in high-energy collisions. The bonding properties of the various species and the energetics of the associated electron-transfer processes can in turn be investigated by means of *ab initio* quantum chemical calculations at a reasonable level of theory.

II. EXPERIMENTAL AND COMPUTATIONAL DETAILS

The experiments were performed with a VG ZAB/HF/AMD 604 four-sector mass spectrometer of *BEBE* (*B* stands for magnetic and *E* for electric sectors) configuration which has been described elsewhere.[13] The XeX[+] ions were generated either by electron ionization (i.e., XeF_2 for XeF[+]) or by chemical ionization of the appropriate precursor mixtures (i.e., Xe/NF_3 for XeF[+], Xe/Cl_2 for XeCl[+], Xe/1,2-dibromoethane for XeBr[+], and Xe/CH_2I_2 for XeI[+]), accelerated to 8 keV translational energy, and mass selected at resolutions of $m/\Delta m\approx 2000-4000$.

In addition to experiments at increased mass resolution, collisional-activation (CA) spectra (helium, 80% transmission, T) were recorded for all the ions of interest in order to probe the presence of interfering isobaric ions. Except for XeCl[+], the CA spectra were unambiguously assigned to the respective XeX[+] ions, showing only signals corresponding to Xe[+] and X[+] as well as small amounts of dications formed by charge stripping of the monocations,[14] e.g., XeX[2+] and Xe[2+]. Unfortunately, in the case of XeCl[+], some interferences due to formation of $C_2H_nCl_4^+$ ($n=0-2$) ions were always observed, even when a Xe/Cl_2 mixture[14] was used as a precursor indicating some contamination in the inlet system of our mass spectrometer. Separation of the XeCl[+] signals from these interferences could, however, be optimized by increasing the resolution of the instrument in combination with a proper choice of the xenon isotope, i.e., for the mixture of $^{132}Xe\,^{35}Cl^+$ and $^{130}Xe\,^{37}Cl^+$ isotopes ($m/z=167$) the interferences were less than 1%. Further, when a Xe/NF_3

mixture is used as precursor for XeF$^+$, the ^{129}XeF$^+$ isotope was mass selected, because all other XeF$^+$ signals overlap with XeOH$^+$ isotopes, probably due to the occurrence of the exchange reaction[15] XeF$^+$+H$_2$O→XeOH$^+$+HF with background moisture in the ion source.

For NR experiments, which involve neutralization of cations and subsequent reionization to cations (indicated as $^+$NR$^+$), the XeX$^+$ ions were selected using the first two sectors $B(1)$ and $E(1)$, then neutralized by collision with xenon ($80\% T$), after which the remaining ions were removed from the beam by applying a high voltage to a deflector plate. The remaining beam of fast neutrals was submitted to reionization by collision with molecular oxygen ($80\% T$), and the resulting fragment-ion mass spectra were recorded by scanning $B(2)$.

The XeF$^+$ cation was also subjected to a NR experiment which involves an inversion of charge[12] (to be referred as $^+$NR$^-$). To this end, $B(1)$-mass selected XeX$^+$ ions were mass selected with $B(1)$, neutralized by collision with xenon ($80\% T$), and after deflection of the remaining ions the neutrals were reionized in a second collision with xenon ($80\% T$), while the negative ions formed were monitored by scanning $E(1)$. Charge-reversal ($^+$CR$^-$) spectra were obtained under identical conditions except that the deflector electrode was grounded. In addition, the energy deficits ΔE_{NR} and ΔE_{CR} for the charge inversion processes have been determined from the high energy onsets of the parent ion and the charge-reversed signals using the energy balance of the process O$_2^{+\bullet}$+2Xe→O$_2^{-\bullet}$+2Xe$^{+\bullet}$ as a reference for the energy scale.[16]

Potential energy curves of the three charge states for each of the XeX species were determined at the coupled cluster level of theory with explicit inclusion of single- and double excitations, and with perturbative treatment of triples [CCSD(T)]. These calculations were performed using MOL-PRO 96,[17] and the spin restricted coupled-cluster code for open-shell species.[18]

For xenon, the relativistic effective core potential (RECP) of Nicklass *et al.* was used to treat the innermost 46 electrons.[19] The valence 5s and 5p electrons were described using the associated $(6s6p3d1f)/[4s4p3d1f]$ basis set. For fluorine and chlorine, the all-electron aug-cc-pVTZ basis sets of Dunning *et al.*[20] were used. These basis sets include diffuse and polarization functions, and are, respectively, of $(11s6p3d2f)/[5s4p3d2f]$ and of $(16s10p3d2f)/[6s5p3d2f]$ size. For bromine, the basis set was based upon the $(17s13p6d)/[6s5p2d]$ set of Schäfer *et al.*[21] This was extended by two diffuse s, p, and d functions (exponents: 0.065, 0.025; 0.04, 0.015; 0.4, 0.15, respectively) and two f polarization functions (0.5, 0.2) to yield a basis set of $(19s15p8d2f)/[8s7p4d2f]$ size. Finally, for iodine, the RECP of Bergner *et al.* was used to treat the innermost 46 core electrons,[22] and the 5s and 5p valence electrons were treated using a $(14s12p9d4f)/[3s3p2d1f]$ basis set.[23] Additionally, core polarization effects were taken into account for iodine using core polarization potentials (CPPs) as implemented in MOLPRO.[17] This combination of basis sets and RECPs is referred to in the text as BSI. In all CCSD(T)

calculations, the HF orbitals of the ''core'' electrons were treated as frozen cores.

For the heavier elements Xe, Br, and I the effect of spin–orbit coupling on open-shell states is non-negligible. Therefore, the calculated energies for separated Xe$^{+\bullet}$, Br$^{+/\bullet}$, and I$^{+/\bullet}$ were empirically corrected according to the J-weighted spin–orbit levels as determined by spectroscopic means.[24] For the neutral XeX$^\bullet$ radicals, the weak van der Waals interactions were to a first approximation assumed not to modify the spin–orbit splitting of the free X atoms (X =Br, I).[6,7,24] The bond energies calculated using the RCCSD(T) method as previously described were therefore used without any further corrections. Vibrational frequencies of the neutrals were generally not considered explicitly in our calculations, because these are already known quite accurately from spectroscopy,[5–7] and we cannot expect the applied level of theory to give very accurate results for the weak and anharmonic potentials of the XeX$^\bullet$ species.

For neutral XeF$^\bullet$, the potential energy curve was studied with other methods and other basis sets. Multireference averaged coupled-pair functional (MR-ACPF) calculations[25] were performed, in which the orbitals were first optimized in a complete active space self-consistent field (CASSCF) calculation including all electrons on fluorine and the eight valence electrons on xenon, in the corresponding orbitals. This active space also includes the important charge-transfer configuration [Xe$^{+\bullet}$F$^-$]. ACPF calculations were then performed including all CAS determinants in the reference space, so that no electrons were frozen. Although it would be more correct to maintain the F 1s orbital doubly occupied in the CAS calculation and frozen in the ACPF treatment,[26] slight irregularities in the potential-energy curves were observed when this was done, presumably due to small rotations between the closed F 1s orbital and the active-space valence orbitals during the orbital optimization. The ACPF expansion was optimized with reference to two roots, in order to properly treat the mixing-in of the charge-transfer configuration. The calculations were performed both with BSI and BSII. Here, BSII stands for an expansion of BSI in the following way. For xenon, one set each of diffuse s, p, and d functions (exponents: 0.03, 0.02, 0.05) was added, the single f function was replaced by three f primitives (1.375, 0.55, 0.22), and one g function (0.55) was added, to yield an overall basis set of $(7s7p4d3f1g)/[5s5p4d3f1g]$ size. For fluorine, the standard aug-cc-pVQZ basis set was used and extended by one set each of extra-diffuse s, p, and d primitives (0.034 376, 0.026 272, 0.0828), thus giving an overall $(14s8p5d3f2g)/[7s6p5d3f2g]$ contraction. Although the ACPF method is approximately size consistent, to obtain precise results for this very weakly bonded molecule, the bond energy at the ACPF level was calculated from the supermolecule (r=50 Å).

The effects of spin–orbit coupling were treated using an approximate one-electron spin–orbit Hamiltonian,[27] as implemented in the GAMESS for PC program.[28] For Xe, the innermost 46 electrons were treated using the RECP of Stevens *et al.*[29] with the associated valence basis set. This basis set was extended by s and p diffuse functions (0.033 944 each), by three d polarization functions (1.0, 0.4,

0.16), and one f polarization function (0.45), which were optimized at the CISD level. For fluorine, the GAMESS TZV basis set was used, extended by s and p diffuse functions (0.1076 each) and two d polarization functions (1.8, 0.45). Due to program limitations, all $6d$ and $10f$ Cartesian components of the polarization functions were maintained. Complete-active-space self-consistent field (CASSCF) orbitals were optimized in a state-averaged approach for the $^2\Sigma^+$ ground state and the degenerate $^2\Pi$ first excited state of XeF$^\bullet$. As above, the CAS space included all occupied orbitals. Using the CAS orbitals, the first six roots of a configuration-interaction (CI) expansion, which included all of the CAS configurations and all determinants formed by single excitations into the external orbitals (FOCI wave function), were calculated. These roots correspond to the ground and excited $^2\Sigma^+$ states and to the ground and excited degenerate $^2\Pi$ states of the XeF$^\bullet$ molecule. At this level, the ground state has a very shallow minimum corresponding to those of the CCSD(T) and MR-ACPF curves.[30] Thereafter, the spin–orbit coupling matrix elements between all the spin substates of these six roots were calculated using the approximate one-electron operator, and the values obtained were used to obtain six nondegenerate spin–orbit coupled eigenstates. The effective nuclear charges used were of 6507 for xenon and 6.2 for fluorine, these values were chosen to reproduce the experimental splittings for F$^\bullet$ (^2P) and Xe$^{+\bullet}$ (^2P) in calculations using analogous FOCI wave functions. The difference in total energy between the first root of the nonrelativistic FOCI calculation and that of the spin–coupled calculation was used to correct the MR-ACPF potential-energy curve of the ground state for spin–orbit coupling. The potential-energy curves obtained at various levels for neutral XeF$^\bullet$ were used to derive vibrational frequencies. These were calculated with the VIBROT routine of the MOLCAS program package,[31] by solving the full rovibrational Schrödinger equation on a cubic spline fit to the calculated points on the potential-energy curve, and thus explicitly includes anharmonicity.

The NBO population analysis of the neutral and ionic species was performed with the NBO program as implemented in GAUSSIAN94.[32,33] The required density was in each case obtained from the corresponding UMP2 wave function at the CCSD(T)/BSI optimized minimum, using the standard LANL2DZ basis set for all atoms, to which even-tempered s and p diffuse functions as well as one d polarization function was added on all atoms. With the LANL2DZ basis set, the core electrons are treated by the RECP of Hay and Wadt, except for fluorine which is treated in an all-electron ansatz. Tests for XeF$^\bullet$ indicated that the use of larger basis sets and/or better correlation treatment did not lead to different charge distributions.

III. RESULTS

In this section we shall describe the experimental and theoretical results and also discuss some conclusions which are either obvious from the experiments or can be derived from a comparison of the theoretical results with previous experimental and/or theoretical studies.

TABLE I. Ion intensities (base peak=100) in the $^+$NR$^+$ spectra (Xe, 80% T; O$_2$, 80% T) of XeX$^+$ ions with X=F, Cl, Br, and I.

	XeX^{+a}	Xe$^{+\bullet}$	X^{+b}
XeF$^+$	100	8	<1
XeCl$^+$	3^c	100	4
XeBr$^+$	<1	100	20
XeI$^+$	3	100	70

[a]In order to ascertain the identity of the recovery signals, several isotopes have been examined, e.g., ^{129}XeX, ^{131}XeX, and ^{132}XeX.

[b]The increase of the X$^+$ signals from F to I is due to the decreasing ionization energies of the halogen atoms and increasing collection efficiencies for the heavier elements.

[c]Due to minor interferences with C$_2$H$_n$Cl$_4^+$ (n=0–2), the identity of the recovery signal remains somewhat uncertain.

A. Experiment

The neutralization-reionization mass spectra of XeX$^+$ cations reveal quite different behaviors of the four xenon halides (Table I). Thus, the $^+$NR$^+$ spectra of XeX$^+$ for X=Cl, Br, and I are quite comparable in having small recovery signals for XeX$^+$, and Xe$^{+\bullet}$ as the base peak, while the XeF$^+$ cation behaves in a strikingly different way. With respect to the corresponding Xe$^{+\bullet}$ signals, the amount of XeX$^+$ recovery signals is more than two orders of magnitude more intense for X=F than for X=Cl, Br, and I. The recovery signals due to reionization of the neutral species are particularly small for X=Cl as well as Br and may in part, or even completely, be due to isobaric interferences. The identity of the recovery signals in the $^+$NR$^+$ spectra of XeF$^+$ and XeI$^+$ is, however, beyond any doubt, clearly demonstrating that both species have long-lived neutral counterparts. Due to the design of the experimental setup,[12,13] it follows that the neutral XeX$^+$ species with X=F and I exhibit lifetimes of at least a few microseconds which are long enough to ensure energy randomization in the neutrals rather than probing the excitation of specific modes.

The large difference of the intensities of the recovery signals implies that there exists a fundamental difference between XeF$^\bullet$ and the other neutral xenon halides, which could, for example, be an unusually large stability of XeX$^\bullet$ for X=F as compared to X=Cl, Br, and I. However, such a result in itself cannot be conclusive. Two other possibilities have to be considered: (i) the four xenon halides may exhibit very different Franck–Condon factors which are known to be extremely important in NR experiments in which vertical electron transfer occurs,[12,34] and (ii) the recovery signal due to the formation of neutral XeX$^\bullet$ may actually be generated by the ionization of the tightly bound excimers XeF$^\bullet$ ($2\,^2\Sigma^+$) and XeF$^\bullet$ ($2\,^2\Pi$). The latter hypothesis is, however, rather unlikely to account for the intense recovery signal corresponding to XeF$^\bullet$ with a lifetime of at least a few microseconds, because it is well known—and also important for their function in excimer lasers—that the excited charge-transfer states exhibit lifetimes in the nanosecond regime.[4,35] Beyond the mere existence of a neutral species with a lifetime of at least a few microseconds, the $^+$NR$^+$ experiments cannot, however, provide any further information about a diatomic species. Additional information can be extracted from NR

experiments in which the charge of the projectile ion is inverted. In the $^+\text{NR}^-$ mass spectrum of XeF^+ a recovery signal corresponding to XeF^- anion formed by reionization of transient neutral $\text{XeF}^\bullet$ is indeed observed as the base peak along with the F^- fragment. A $^+\text{NR}^-$ event with neutral xenon as the target gas can be described in terms of

$$\text{XeF}^+ + \text{Xe} \rightarrow \text{XeF}^\bullet + \text{Xe}^{+\bullet}, \tag{1}$$

$$\text{XeF}^\bullet + \text{Xe} \rightarrow \text{XeF}^- + \text{Xe}^{+\bullet}. \tag{2}$$

Reactions (1) and (2) involve electron-transfer processes from the xenon target to the fast-moving XeF molecule. Both reactions are quite endothermic and can be assumed to proceed as vertical transitions driven by the translational energy of the projectile. The energy required for the formation of a $^+\text{NR}^-$ recovery signal is provided by the translational energy and leads to a shift of the recovery signal to slightly lower kinetic energies as compared to the parent ion. To a first approximation, this energy difference (ΔE_{NR}) can be estimated as $\Delta E_{\text{NR}} = \text{Re}_v(\text{XeF}^+) + \text{EA}_v(\text{XeF}^\bullet) - 2\text{IE(Xe)}$, where RE_v stands for the associated (vertical) recombination energy of the cation, EA denotes the (vertical) electron affinity of the transient neutral, and IE is the ionization energy of xenon which was used as a target gas in these experiments. Using the ΔE_{NR} associated with the process $\text{O}_2^{+\bullet} \rightarrow \text{O}_2^{-\bullet}$ as a reference, we obtain $\Delta E_{\text{NR}}(\text{XeF}^+ \rightarrow \text{XeF}^-) = -9.6 \pm 0.7 \text{ eV}$, and thus, $\text{RE}_v(\text{XeF}^+) + \text{EA}_v(\text{XeF}^\bullet) = 14.7 \pm 0.7 \text{ eV}$ with $\text{IE(Xe)} = 12.13 \text{ eV}$. This result is about 1 eV higher than the sum of the adiabatic values taken from the literature, i.e., $\text{RE}_a(\text{XeF}^\bullet) = \text{IE}_a(\text{XeF}^\bullet) = 10.3 \text{ eV}$[36] and the assumption $\text{EA}_a(\text{XeF}^\bullet) \approx \text{EA}(\text{F}^\bullet) = 3.4 \text{ eV}$; a finding which will be addressed in more detail further below. In a charge-reversal experiment from cations to anions ($^+\text{CR}^-$), electron transfer may either occur in a stepwise manner involving two collisions, or in a single collision, i.e., two single-electron transfers versus one two-electron transfer. We found that ΔE_{NR} and the corresponding ΔE_{CR} are identical within the experimental error, indicating that in charge-reversal experiments, either with or without intermediate neutralization, the same sequence of reactions (1) and (2) occurs at threshold. Instead, a direct two-electron transfer according to reaction (3) would be associated with a significantly larger energy deficit, because the second ionization energy of xenon is about 9 eV larger than the first one,

$$\text{XeF}^+ + \text{Xe} \rightarrow \text{XeF}^- + \text{Xe}^{2+}. \tag{3}$$

Another interesting aspect arises from the comparison of the $^+\text{CR}^-$ and $^+\text{NR}^-$ mass spectra of XeF^+ which were obtained under identical collision and focusing conditions, except that the deflector electrode was grounded in the $^+\text{CR}^-$ experiment. Both spectra are rather simple and besides XeF^- only F^- is observed as an anion fragment. The XeF^- anion represents the base peak in both spectra, but interestingly the ratio of the XeF^- and F^- fragments is lower in the $^+\text{CR}^-$ ($\text{XeF}^-/\text{F}^- = 100:60$) than in the $^+\text{NR}^-$ spectrum ($\text{XeF}^-/\text{F}^- = 100:30$). According to some recently outlined criteria,[37] the neutral and ion decomposition difference (NIDD) scheme, such an increase of the recovery signal relative to the fragments in $^+\text{NR}^-$ versus $^+\text{CR}^-$ indicates the

TABLE II. Calculated and experimental electron affinities (EA in eV) of the halide radicals $X^\bullet$ at the CCSD(T)/BSI level of theory.[a,b]

	EA_{calc}	EA_{exp}[c]
F	3.30	3.40
Cl	3.47	3.62
Br	3.15	3.36
I	2.62	3.06

[a]With a correction for the experimental spin–orbit coupling.
[b]For details, see computational section.
[c]Taken from Ref. 36.

occurrence of some energy redistribution and reorganization in the intermediate neutral which increases the Franck–Condon factors for reionization to the opposite charge in the NR scheme. This does not, of course, occur in the CR experiment. Thus, stepwise electron transfer to XeF^+ in the $^+\text{NR}^-$ process involving a microsecond lifetime of the neutral is more efficient than direct two-electron transfer or sequential electron transfer within shorter periods which are primarily sampled in $^+\text{CR}^-$ experiments.

B. Theory

The mass-spectrometric experiments described involve vertical transitions between the anionic, neutral, and cationic potential-energy curves, and it is important to know how much energy this demands, and how much will be deposited in the product species in these electron-transfer processes. Because there are no uniform potential-energy curves for the three charge states available, we decided to calculate them using *ab initio* molecular orbital (MO) calculations, using coupled-cluster calculations with large, triple-zeta polarized basis sets. This level of theory should give reasonably accurate results, even for rather demanding properties such as ionization energies and electron affinities. This is supported by the data in Table II, which show good agreement between calculated and experimental electron affinities for the halogen atoms. As discussed below, the calculated potential-energy curves for the three charge states of the four xenon monohalides are also in reasonable agreement with experimental data, where available. They are therefore presumed to be adequate for the discussion of our experimental results.

More extensive calculations were performed for the neutral XeF species, for several reasons. First, the initial calculated curve was only in moderate agreement with the available experimental data; second, this is experimentally one of the most extensively investigated of the present species; third, despite the experimental interest, there were no previous high-level *ab initio* data on this diatomic; and fourth, it appeared useful to ascertain to which effects the potential-energy curve is sensitive, as a reference for future *ab initio* studies of this and other similar species.

The XeX^+ cations exhibit singlet ground states and display reasonably strong chemical bonds,[38] formally due to electron coupling between $\text{Xe}^{+\bullet}$ (^2P) and $X^\bullet$ (^2P). Along the halogen row the dissociation energies with respect to the $\text{Xe}^{+\bullet} + X^\bullet$ asymptotes increase from fluorine to iodine (Table III). From a chemical point of view this trend indicates a charge-transfer stabilization due to mixing of the configura-

TABLE III. Bond lengths (in Å) and dissociation energies (in kcal/mol) of xenon halides in various charged states calculated with the CCSD(T) method and basis set I (BSI) as described in the computational details. The dissociation energies are given relative to the respective dissociation asymptotes, i.e., $Xe^+ + X^\bullet$ for the cations,[a] $Xe + X^\bullet$ for the neutrals, and $Xe + X^-$ for the anions. The available experimental values are given for comparison.

		r_e (Å)	D_e (kcal/mol)	Experimental values
XeF	Cation	1.89	46.3	$D_0 = 46.2$ kcal/mol[36]
	Neutral	2.41	1.8	$r_e = 2.29$ Å, $D_e = 3.0$ kcal/mol[e]
		[2.31][b]	[3.0][b]	
	Anion	3.01	5.5	
XeCl	Cation	2.34	50.3	
	Neutral	3.43	1.0	$r_e = 3.23$ Å, $D_e = 0.8$ kcal/mol[f]
	Anion	3.80	2.8	$r_e = 3.81$ Å, $D_e = 3.1$ kcal/mol[g]
XeBr	Cation	2.50	53.8 (43.7)[c]	
			46.5[d] (40.2)[c,d]	
	Neutral	3.67	1.1	$r_e = 3.85$ Å, $D_e = 0.7$ kcal/mol[h]
	Anion	4.01	2.4	$r_e = 3.62$ Å, $D_e = 3.3$ kcal/mol[g]
XeI	Cation	2.71	59.9 (49.8)[c]	
			21.1[d] (12.4)[c,d]	
	Neutral	4.16	0.6	$r_e = 4.05$ Å, $D_e = 0.8$ kcal/mol[h]
	Anion	4.34	2.3	

[a]For X=Br and I the lowest dissociation asymptotes of XeX^+ correspond to the adiabatic dissociation into $Xe(^1S) + X^+(^3P)$ involving the triplet surface.

[b]Calculated at a higher level of theory, i.e., MR-ACPF+SOC with BSII; see the text.

[c]Bond energies corrected for the experimental spin–orbit coupling of the corresponding asymptote.

[d]Dissociation into $Xe(^1S) + X^+(^3P)$ as derived from the differences in the experimental ionization energies taken from Ref. 36.

[e]Reference 5(d).

[f]Reference 7.

[g]Reference 11.

[h]Reference 6.

tions $Xe^+ - X \leftrightarrow Xe - X^+$ such that D_e increases with decreasing ionization energy (IE)[36] of the halogen, i.e., $IE(F^\bullet) = 17.42$ eV, $IE(Cl^\bullet) = 12.97$ eV, $IE(Br^\bullet) = 11.81$ eV, and $IE(I^\bullet) = 10.45$ eV, and $IE(Xe) = 12.13$ eV. In complete agreement with this phenomenological description of bonding in the XeX^+ cations, the population analysis predicts partial charges on the xenon in XeX^+ which monotonically decrease from X=F to X=I (Table IV). In fact, the charge of 1.335 in XeF^+ indicates a charge-transfer resonance of the type $Xe^+ - X \leftrightarrow Xe^{2+} - X^-$ in the case of the xenon fluoride cation.[38] The trend for increasing D_e is, however, partially compensated by two effects, namely relativity and changes of the dissociation behavior. Thus, the strong spin–orbit coupling (SOC) in the free halogen atoms $Br^\bullet$ and $I^\bullet$ lowers the $Xe^{+\bullet} + X^\bullet$ dissociation asymptotes for these halogens while to a first approximation SOC can be neglected in the singlet ground states of the XeX^+ molecules. Further, the IEs of

TABLE IV. Calculated charges on xenon in the $XeX^{+/\circ/-}$ species (X=F, Cl, Br, and I) according to natural orbital population analysis.

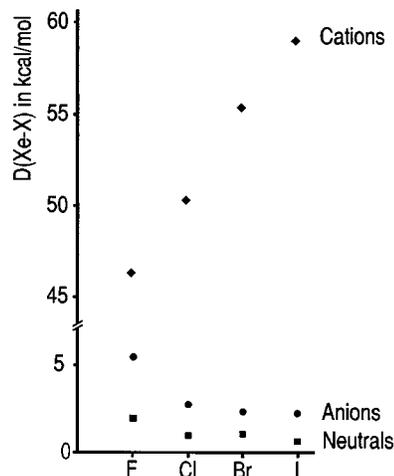|	Anion	Neutral	Cation
XeF	0.001	0.200	1.335
XeCl	0.000	0.022	0.896
XeBr	−0.001	0.016	0.762
XeI	−0.001	0.006	0.601

FIG. 1. Calculated bond dissociation energies of $XeX^{+/\circ/-}$ (X=F, Cl, Br, I) relative to the $Xe^+ + X$ asymptote for the cations (◆), the $Xe + X$ asymptote for the neutrals (■), and the $Xe + X^-$ asymptote for the anions (•). Note the break in the energy axis.

bromine and iodine are lower than that of xenon so that the $Xe(^1S) + X^+(^3P)$ channel represents the lowest dissociation asymptote for these two halogens, involving also a crossover from the singlet to the triplet surface en route to dissociation.

Quite different trends are obtained for the neutral and anionic species in which the xenon fluorides are significantly more strongly bound than the other xenon halides (Fig. 1). Nevertheless, all bonds are fairly weak and these diatomic molecules can hardly be expected to be observable at thermal energies. The exceptional stability of neutral $XeF^\bullet$ has been described previously[5,7] and attributed to charge-transfer stabilization involving the configurations $Xe - X^\bullet \leftrightarrow Xe^{+\bullet} - X^-$, which is most pronounced for X=F (see below). Instead, neutral $XeBr^\bullet$ and $XeI^\bullet$ can be described in terms of pure van der Waals interactions; $XeCl^\bullet$ is somewhat in-between, but also dominated by van der Waals forces. The decrease of $D_e(Xe - X^-)$ in the anions is straightforward in that dispersion is simply maximized for the small fluoride anion as the binding partner and then decreases with the size and charge density of the halide going down the periodic table. As far as the bond lengths are concerned, these nicely follow the qualitative trends derived from the dissociation energies. Thus, r_{Xe-X} is always the smallest for X=F and r_{Xe-X} also increases from the cations to the neutrals and then to the anions, i.e., the cations exhibit a short, covalent bond, dispersion dominating in the neutrals, and additional bond elongation is caused by electron repulsion in the anions. Nevertheless, the dissociation energies of the anions exceed those of the neutrals, because in the former ion/induced dipole forces are present while in the neutrals only induced polarizability comes into play.

Comparison of the present theoretical results with the experimental values available is quite satisfactory and demonstrates that the performance of the theoretical approach chosen is acceptable for more than a qualitative description of van der Waals complexes such as the $XeX^\bullet$ molecules. Thus, the experimental and theoretical bond energies agree to within ±1 kcal/mol, which is certainly also the limit of

J. Chem. Phys., Vol. 108, No. 20, 22 May 1998

Schröder *et al.*   8451

TABLE V. Calculated energies (in eV) for some vertical electron transfer processes of $XeF^{+/\circ/-}$ species.

Electron transfer process	Vertical	Adiabatic	Excitation[a]
$XeF^+ \rightarrow XeF^\bullet$	−9.4	−10.3	0.8
$XeF^\bullet \rightarrow XeF^+$	11.5	10.3	1.3
$XeF^- \rightarrow XeF^\bullet$	3.6	3.5	0.1
$XeF^\bullet \rightarrow XeF^-$	−3.2	−3.5	0.3
$XeCl^+ \rightarrow XeCl^\bullet$	−8.9	−10.0	1.1
$XeCl^\bullet \rightarrow XeCl^+$	11.8	10.0	1.8
$XeBr^+ \rightarrow XeBr^\bullet$	−8.8	−9.9	1.1
$XeBr^\bullet \rightarrow XeBr^+$	11.7	9.9	1.8
$XeI^+ \rightarrow XeI^\bullet$	−8.4	−9.6	1.2
$XeI^\bullet \rightarrow XeI^+$	11.3	9.6	1.7

[a]This column is the absolute value of the difference in energy between vertical and adiabatic electron transfer, which can be regarded as the amount of internal energy deposited in the species upon formation by vertical electron transfer from the ground state of the respective precursor state.

TABLE VI. Comparison of bond lengths (r in Å), dissociation energies (D_e in kcal/mol), and frequencies (ω in cm^{-1}) for the $^2\Sigma^+$ ground state of neutral $XeF^\bullet$ calculated at different levels of theory.

Level of theory[a]	r	D_e	ω
CCSD/BSI	3.04	0.5	28
CCSD(T)/BSI	2.425	1.7	138
CCSD/BSII	3.06	0.6	16
CCSD(T)/BSII	2.375	2.1	152
MR-ACPF/BSI	2.35	2.4	178
MR-ACPF/BSII	2.316	2.7	191
MR-ACPF+SOC/BSII	2.31	3.0(1.8)[b]	206

[a]See computational details.
[b]The value in brackets includes the corrections for the basis set superposition error which is primarily due to an insufficient description of the xenon atom.

confidence for our CCSD(T) calculations. A notable exception is, however, the $XeF^\bullet$ radical for which these initial calculations yields predictions of $r_e = 2.40$ Å, $D_e = 1.8$ kcal/mol, and $\nu = 133$ cm^{-1}, thus indicating a significant underestimation of the attractive interaction regarding the experimental values[5(d)] of $r_e = 2.29$ Å, $D_e = 3.0$ kcal/mol, and $\nu = 225$ cm^{-1}. To understand the origin of this effect, we performed supplementary calculations which are described below (see Table V).

With regard to the mass spectrometric experiments, the vertical transitions from the various charged states into the others are also of interest. Due to the fact that the differences of the equilibrium distances in the cations, neutrals, and anions are significant, Franck–Condon factors become important, and one can expect that the energy requirements of vertical and adiabatic electron-transfer processes will differ significantly. As far as the $^+NR^+$ experiments are concerned, vertical neutralization of the ground state cations deposits a significant amount of excess energy in the neutrals as revealed by the comparison of the vertical and adiabatic energetics associated with neutralization of the cations. Similarly, the differences between the vertical and adiabatic ionization of the neutrals to the cations are significant. Regarding the dissociation energies of the neutral $XeX^\bullet$ radicals, long-lived neutrals can therefore only be formed from vibrationally excited states of the precursor ions (see below). Notwithstanding, these effects are not dramatically different from one halide to another. Though the changes are less pronounced for X=F, Franck–Condon factors alone cannot account for the large difference between the $^+NR^+$ spectra of XeF^+ as compared to the other xenon-halide cations. Due to the smooth potentials of neutral $XeF^\bullet$ and the XeF^- anion, the energetics of adiabatic and vertical electron transfer are less different and readily account for the observation of a recovery signal in the $^+NR^-$ spectrum of XeF^+.

As stated above, the CCSD(T)/BSI calculations performed for the neutral $XeF^\bullet$ radical gave only moderate agreement with the experimental data. We therefore explored the possible causes of these deficiencies, through some supplementary calculations. First, the effect of enlarging the

basis set was considered by recalculating the potential-energy curve at the CCSD(T) level, using the enlarged basis set BSII. This treatment does indeed lead to a slight improvement of the results (Table VI). However, it was observed with both basis sets that the CCSD curve only displays a very weak minimum at high interatomic separation, characteristic of a van der Waals-type interaction. This large difference between the CCSD and CCSD(T) results suggests that the coupled-cluster theory does not adequately describe the bonding situation in $XeF^\bullet$, presumably due to some multi-configurational character of the wave function.[39] We therefore recalculated the potential energy curve with both basis sets at the multireference averaged coupled-pair functional (MR-ACPF) level, which treats the mixing of the Xe–$F^\bullet$ and $Xe^{+\bullet}$–F^- configurations in a more adequate way. In fact, the MR-ACPF treatment leads to sizable increases of the bond energies and vibrational frequencies, much more significant than the basis set effect (Table VI). Further, the effect of basis-set superposition error (BSSE) was estimated using the counterpoise method at the equilibrium geometry of $XeF^\bullet$. Though the BSSE of about 1.2 kcal/mol is not too large, it is quite unbalanced and primarily due to the description of the xenon atom, indicating that the corresponding basis set is still far from saturated.

Even with the MR-ACPF method and the very large BSII, the agreement with experiment is still not perfect. In part, this is certainly due to remaining deficiencies in the one-particle and two-particle spaces. However, another effect which should be taken into account is spin–orbit coupling, due to the minor contribution of the $Xe^{+\bullet}$–F^- configuration. With the large nuclear charge for xenon, spin–orbit coupling is expected to lead to extensive mixing of the $^2\Sigma^+$ configuration ($J = 1/2$) with the $J = 1/2$ component of the $^2\Pi$ configuration, and consequently to a stabilization of the ground state. To estimate this effect, we incorporated a spin–orbit correction to the MR-ACPF curve. This correction was derived from spin–orbit calculations along the whole curve, using an approximate one-electron operator.[27] First, normal spin–orbit free CI wave functions were generated for the ground and excited $^2\Sigma^+$ and $^2\Pi$ states, then the SO matrix elements between these states were computed using the one-electron operator, and finally the spin–orbit Hamiltonian was diagonalized using the CI energies and spin–orbit coupling
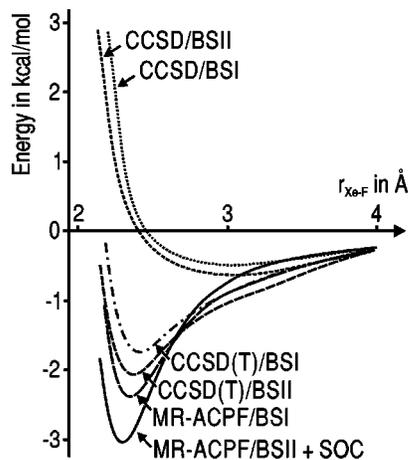
FIG. 2. Potential-energy curves for the XeF$^\bullet$ molecule with different methods and basis sets.

constants, to give a set of six nondegenerate curves for the four lowest states of $J=1/2$ and two lowest states of $J=3/2$. The stabilization of the ground state induced by spin–orbit coupling derived from these CI calculations was then added to the MR-ACPF results to yield the spin–orbit corrected curve (Fig. 2). As can be seen, the effect of this correction is to slightly increase the bond energy and decrease the bond length of the ground state molecule. This last effect is due to the fact that at shorter distances, the ionic configuration contributes more, thus there is more spin–orbit coupling and the ground state experiences more stabilization. The occurrence of significant charge transfer is illustrated by the large magnitude of the coupling constant between the ground $^2\Sigma^+$ state and the charge-transferred excited $^2\Pi$ state, which amounts to 1860 cm^{-1} at the minimum. This very high value can only be obtained if the ground state has significant Xe$^{+\bullet}$ character. Finally, this treatment leads to a theoretical prediction of $r_e=2.31$ Å, $D_e=3.0$ kcal/mol, and $\nu=206$ cm^{-1}, which compares favorably with the experimental values[5(d)] of $r_e=2.29$ Å, $D_e=3.0$ kcal/mol, and $\nu=225$ cm^{-1}.

To conclude, it is possible to obtain reasonable agreement with experiment for the spectroscopic data of the xenon halide species at the CCSD(T) level of theory. However, this approach still contains many limitations which are most apparent for the neutral XeF$^\bullet$. Our study shows that a fully reliable treatment of the rather weak interaction of neutral xenon and fluorine atoms requires a multireference approach, with a good treatment of correlation as well as very large basis sets, and explicit consideration of scalar– and spin–orbit relativistic effects. Clearly, a treatment at this level is still somewhat elusive at the current point in time, because although the present calculations address all of these points, they incorporate some approximations (use of an RECP and of the one-electron spin–orbit operator) and are still far from being converged with respect to the full CI and infinite basis set limits.

IV. DISCUSSION

The experimental data described above demonstrate that neutral XeF$^\bullet$ and XeI$^\bullet$ having at least microsecond lifetimes

can be generated in NR experiments, while the nature of the recovery signals due to reionized XeCl$^\bullet$ and XeBr$^\bullet$ is much more vague. In order to provide a rationale of the different behavior of the neutral xenon(I) halides, a discussion of the experimental findings in light of previous results and the present theoretical studies is indicated.

Let us first address the possibility that the neutral species formed are the charge-transfer excimer states [Xe$^+$–F$^-$] and not the weakly bound, van der Waals-type ground state molecules XeX$^\bullet$. Above, we have claimed that these excimers cannot explain the observation of recovery signals in the NR experiments due to their very short lifetimes in the nanosecond regime,[4] while the NR method samples the microsecond time frame. Further, comparison of the lifetimes of XeX$^\bullet$ for X=F–I reported in Ref. 4 reveals nothing particular for XeF$^\bullet$. Nevertheless, the lifetime argument remains somewhat vague, and more detailed consideration with respect to geometrical parameters is indicated. Detailed information about the excimer states is available, and for all halides except XeF$^\bullet$, the bond length r_{Xe-X} is larger in the ground state than in the excimer states. For XeF$^\bullet$, however, r_{Xe-X} is larger in the excimers (2.49 Å)[4,40] than in the ground state (2.29 Å)[5(b)] and this highlights a fundamental difference which may account for the different NR results. In fact, in the case of fluorine, formation of the excimer state would therefore lead to a neutral in which electron transfer to the anion will be more favorable due to the increase of r_{Xe-X}; i.e. the $^+$NR$^-$ experiment proceeds as XeF$^+$→[Xe$^{+\bullet}$–F$^-$]→XeF$^-$, rather than involving the ground state. This would indeed indicate an exceptional situation for xenon fluoride in the $^+$NR$^-$ experiment. Further, this scenario cannot be distinguished by means of the energy deficit ΔE_{NR} from the one involving a passage through the ground state of the neutral, because the overall energy balance of both processes is identical, i.e., XeF$^+$+2e^-→XeF$^-$. On the other hand, the same r_{Xe-X} argument would predict a *lower* yield of the recovery ion in the $^+$NR$^+$ experiments with XeF$^+$ as compared to the excimer states of the other xenon halides which have geometries matching closer that of the corresponding cations. Since precisely the opposite is observed experimentally, the r_{Xe-X} argument appears less important, further supporting the formation of ground state XeF$^\bullet$ in the NR experiments. Finally, if one compares the $^+$CR$^-$ and $^+$NR$^-$ spectra, one notes that the recovery signal is *larger* for the longer lived neutrals, which does not agree with the formation of excimers having a limited lifetime.[4] To summarize all these arguments, we conclude that the NR experiments lead to genuine neutral XeF$^\bullet$ in its $^2\Sigma^+$ ground state, i.e., a species trapped in a potential-energy well of a few kcal/mol is formed by vertical electron transfer in a kiloelectron volt collision event (see below).

The neutral XeX$^\bullet$ species (X=F, Cl, Br, and I) have already been described in some detail,[5–7] and in this comparative study let us dwell on the essential issues of the present experimental and theoretical results. First, what is special about XeF$^\bullet$ which means that it gives rise to a much more intense recovery signal than the other xenon halides (Table I)? Second, how can a shallow minimum, such as that neutral XeF$^\bullet$, be reached in a collision experiment involving
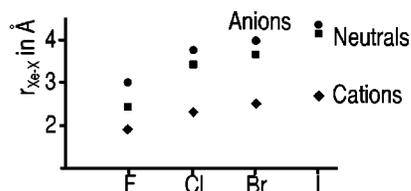
FIG. 3. Calculated bond distances of $XeX^{+/\circ/-}$ (X=F, Cl, Br, I) for the cations ($\blacklozenge$), neutrals ($\blacksquare$), and anions ($\bullet$).
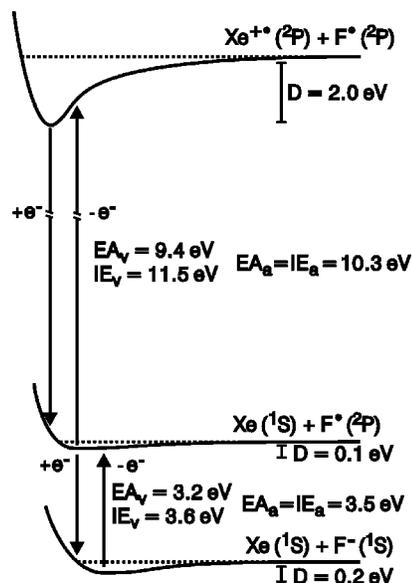

FIG. 4. Schematic potential-energy curves (energies in eV) for the electron transfer events involving cationic, neutral, and anionic xenon fluoride and the respective dissociation channels. The dashed lines indicate the relevant dissociation asymptotes.

ions having kinetic energies in the kiloelectron volt regime? Both questions address not only fundamental issues of neutralization-reionization mass spectrometry, but also of other spectroscopic methods to tackle species trapped in rather small potential-energy wells.

At first sight, neither the structures nor the energetics of the various charge states of the xenon halides display dramatic differences. Thus, all cations exhibit a chemical bond of reasonable strength with respect to the respective dissociation asymptotes, and the bond lengths of the various charge states follow the trends which can be expected along the halogen row. Nevertheless, $XeF^{\bullet}$ resides in a slightly deeper well than the other xenon halides and also in the comparison of the bond length of the cationic, neutral, and anionic species, neutral $XeF^{\bullet}$ is in-between the cations and anions while the other $XeX^{\bullet}$ neutrals are much closer to the anion geometries (Fig. 3). Thus, the nature of the interaction in the xenon fluoride ground state must be qualitatively different from the binding situations in the other xenon halides. Indeed, NBO analysis for X=F and Cl suggest covalent bonding in terms of charge transfer as the origin of this difference in that the partial charge $q_{Xe}(XeF^{\bullet})=0.20$ is much larger than $q_{Xe}(XeCl^{\bullet})=0.02$; similarly, there is a significant spin density on Xe in neutral $XeF^{\bullet}$, while this is almost zero in $XeCl^{\bullet}$. Retrospectively, the computational difficulties observed for $XeF^{\bullet}$, leading to the need to turn to multireferential methods to adequately describe the occurrence of charge transfer, also point to a special nature of $XeF^{\bullet}$ because they were not encountered for the other halides.[41] The large spin–orbit coupling encountered between the ground state of $XeF^{\bullet}$ and some of the excimer excited states also point to significant charge transfer even in the ground state. All in all, these results give qualitative support for the fact that the chemical bonding in $XeF^{\bullet}$ cannot be described only as a van der Waals interaction, but must involve also a degree of polarized covalent character.

After having established this conceptual situation, one wonders how $XeF^{\bullet}$ is formed in the NR experiments. Certainly, mere consideration of the minima cannot suffice for this purpose, because vertical neutralization of ground state XeF^+ deposits ~ 20 kcal/mol in the neutral which is roughly six times more than the binding energy such that dissociation will occur quantitatively well before the end of the microsecond flight time (Fig. 4). In order to understand the energetics of the NR event in which long-lived $XeF^{\bullet}$ is formed, let us therefore consider an extreme case. The minimal distance r_{Xe-F} at which $XeF^{\bullet}$ is still below the dissociation asymptote amounts to about 2.2 Å. At this distance, the vertical electron-transfer process $XeF^+ \rightarrow XeF^{\bullet}$ has an energy balance

of about 10.9 eV. Thus, XeF^+ precursor ions which contain ~ 0.7 eV excess energy may attach an electron from the target gas to yield a stable neutral species. In a similar manner, we can expect a stable XeF^- to be formed upon reionization to anions at a distance of $r_{Xe-F}=2.4$ Å with an energy balance of 3.3 eV for the vertical process $XeF^{\bullet} \rightarrow XeF^-$. Assuming some reorganization of the transient neutral toward longer r_{Xe-F} distances, a threshold of $\Delta E_{NR}=-10.1$ eV is obtained for xenon as the source of the electrons in a $^+NR^-$ experiment. Without this assumption, i.e., r_{Xe-F} in the cation must at least be 2.4 Å to yield a stable anion via stepwise single-electron transfer, ΔE_{CR} calculated as -9.6 eV. These two extreme estimates agree well with the measured values $\Delta E_{CR} \approx \Delta E_{NR}=-9.6 \pm 0.7$ eV and support the proposed sequence of electron-transfer events. Moreover, the assumption of some reorganization of the transient neutral during its passage from one collision cell to the other in the $^+NR^-$ experiment accounts for the increased recovery signal as compared to $^+CR^-$ spectrum. Thus, as the population of excited precursor cations formed in the ion source decreases with increasing excitation energy, a fraction of precursor ions exhibits interatomic distances needed to reach the potential well of the neutral. Instead, only very few will sample the even longer distance required for the direct formation of the XeF^- anion from the corresponding cation in the $^+CR^-$ experiment. Further, within the microsecond time scale of the experiment the neutrals formed by vertical electron transfer to XeF^+ with $r_{Xe-F}=2.2$ Å can experience geometries with longer r_{Xe-F} which hence increases the probability to afford stable XeF^- anions in the reionization event.

Overall, the shallow minimum of the neutral is reached from vibrationally excited XeF^+ cations, and the neutral can reside in its potential-energy well because in the diatomic molecule no other sources of internal energy exist. The same arguments apply for the other xenon halides and the different

behavior of the fluoride may simply be attributed to the slightly deeper well of the neutral. As a result, vertical electron transfer from XeX^+ to yield a neutral with a lifetime of at least a few microseconds is much more likely for $X=F$ than for the other halides. Nevertheless, also in the $^+NR^+$ spectrum of XeI^+ a significant recovery signal is observed. Considering that the minimum of XeI is much more shallow than that of XeF, and that for $X=Cl$ and Br no significant recovery signals are observed, the recovery signal in the case of $X=I$ may indeed be due to formation of minor amounts of the excimer states, for which lifetimes in the range of hundreds of nanoseconds have been reported.[4]

Finally, let us address some implications of this study with respect to the application of neutralization-reionization mass spectrometry probe neutrals resting in rather shallow potential-energy wells. In general, it has been assumed that NR techniques cannot be used to detect weakly bound species such as van der Waals clusters, because the energy deposition in a kiloelectron volt collision is too large to result in species with microsecond lifetimes. The situation is, however, somewhat different for diatomic species such as $XeF^•$. Thus, appropriately excited precursor ions may exhibit geometries close to the minimum structure of the corresponding neutral such that vertical electron transfer can indeed lead to neutrals trapped in quite shallow wells,[42] as demonstrated by the NR experiments with XeF^+. In contrast, for polyatomic systems modes other than the one associated with the appropriate local geometry for vertical neutralization will also store a significant amount of internal energy. Within the microsecond time frame, energy dissipation will occur and thus the excess energy stored in these other modes will lead to dissociation if the binding energy is small. Hence, the empirical concept that van der Waals clusters do not give rise to recovery signals in NR experiments holds true as far as large polyatomic neutrals are concerned, but more detailed considerations are required for small molecules with a few degrees of freedom.

V. CONCLUSION

The previously supposed exceptional thermodynamic stability of the $XeF^•$ radical among the xenon halides has been confirmed by a combined mass-spectrometric and computational approach. Furthermore, the analysis of the nature of the interaction at the equilibrium distance, compared with that in the XeCl species which has been stated to be bound only in a van der Waals sense, strongly support the hypothesis of the occurrence of a covalent interaction.

Two important methodological conclusions can further be drawn from the present study. First, the theoretical methods available today allow an elaborate description of weakly bound systems such as $XeF^•$. Our results do not achieve spectroscopic accuracy, however, especially if one takes into account the effect of BSSE. This is not surprising when one considers the many factors affecting the $XeF^•$ ($^2\Sigma^+$) potential-energy curve: correlation, both nondynamic and dynamic, scalar relativistic effects, and extensive spin–orbit coupling around the minimum. Second, the experimental results demonstrate the ability of neutralization-reionization mass spectrometry to generate long-lived neutrals in rather

narrow potential-energy wells as long as the internal energy content can be kept small enough. Thus, neutral XeF^- can be trapped in its shallow potential-energy well although the neutralization event involves a collision of a precursor ion having a kinetic energy in the kiloelectron volt range.

[1] E. Velazco and D. W. Setzer, J. Chem. Phys. **62**, 1990 (1975).
[2] K. Seppelt and D. Lentz, Prog. Inorg. Chem. **29**, 167 (1982).
[3] For a review on compounds of light noble gases, see G. Frenking and D. Cremer, *Structure and Bonding* (Springer, Berlin, 1990), Vol. 73, p. 17.
[4] T. H. Dunning, Jr. and P. J. Hay, J. Chem. Phys. **69**, 134 (1978); P. J. Hay and T. H. Dunning, Jr., *ibid.* **69**, 2209 (1978).
[5] (a) J. Tellinghuisen, P. C. Tellinghuisen, G. C. Tisone, J. M. Hoffman, and A. K. Hays, J. Chem. Phys. **68**, 5177 (1978); (b) P. C. Tellinghuisen, J. Tellinghuisen, J. A. Coxon, J. E. Velazco, and D. W. Setzer, *ibid.* **68**, 5187 (1978); (c) J. Tellinghuisen, *ibid.* **78**, 2374 (1983); (d) K. Johnson and J. Tellinghuisen, Chem. Phys. Lett. **228**, 363 (1994).
[6] XeBr: J. O. Clevenger and J. Tellinghuisen, J. Chem. Phys. **103**, 9611 (1995); XeI: D. T. Radzykewycz and J. Tellinghuisen, *ibid.* **105**, 1330 (1996).
[7] XeF: C. H. Becker, P. Casavecchia, and Y. T. Lee, J. Chem. Phys. **69**, 2377 (1978); XeCl: V. Aquilanti, D. Cappelletti, V. Lorent, E. Luzzatti, and F. Pirani, Chem. Phys. Lett. **192**, 153 (1992); XeI: P. Casavecchia, G. He, R. K. Sparks, and Y. T. Lee, J. Chem. Phys. **77**, 1878 (1982).
[8] S. P. Mezyk, R. Cooper, and J. G. Young, J. Phys. Chem. A **101**, 2429 (1997); S. Longo, Chem. Phys. Lett. **268**, 306 (1997).
[9] G. F. Adams and C. F. Chabalowski, J. Phys. Chem. **98**, 5878 (1994); J. Styszynski, X. Cao, G. L. Malli, and L. Visscher, J. Comput. Chem. **18**, 601 (1997).
[10] D. E. Riederer, Jr., S. A. Miller, T. Ast, and R. G. Cooks, J. Am. Soc. Mass Spectrom. **4**, 938 (1993); S. D. Price, M. Manning, and S. R. Leone, J. Am. Chem. Soc. **116**, 8673 (1994).
[11] M. G. Thackston, F. L. Eisele, W. M. Pope, H. W. Ellis, E. W. McDaniel, and I. R. Gatland, J. Chem. Phys. **73**, 3183 (1980); D. R. Lamm *et al.*, *ibid.* **79**, 1965 (1983).
[12] Selected reviews about NRMS: A. W. McMahon, S. K. Chowdhury, and A. G. Harrison, Org. Mass Spectrom. **24**, 620 (1989); N. Goldberg and H. Schwarz, Acc. Chem. Res. **27**, 347 (1994); D. V. Zagorevskij and J. L. Holmes, Mass Spectrom. Rev. **13**, 133 (1994).
[13] R. Srinivas, D. Sülzle, T. Weiske, and H. Schwarz, Int. J. Mass Spectrom. Ion Processes **107**, 368 (1991); R. Srinivas, D. Sülzle, W. Koch, C. H. DePuy, and H. Schwarz, J. Am. Chem. Soc. **113**, 5970 (1991).
[14] P. Jonathan, A. G. Brenton, J. H. Beynon, and R. K. Boyd, Int. J. Mass Spectrom. Ion Processes **76**, 319 (1987).
[15] J. E. Huheey, E. A. Keiter, and R. L. Keiter, *Anorganische Chemie* (de Gruyter, Berlin, 1995), Chap. 17.
[16] J. N. Harvey, D. Schröder, A. Fiedler, C. Heinemann, and H. Schwarz, Chem. Eur. J. **2**, 1230 (1996); D. Schröder, C. A. Schalley, J. Hrušák, N. Goldberg, and H. Schwarz, *ibid.* **2**, 1235 (1996); J. N. Harvey, D. Schröder, and H. Schwarz, Bull. Soc. Chim. Belge **106**, 447 (1997).
[17] MOLPRO 96.4 is a package of *ab initio* programs written by H.-J. Werner and P. J. Knowles, with contributions from J. Almlöf, R. D. Amos, M. J. O. Deegan, S. T. Elbert, C. Hampel, W. Meyer, K. Peterson, R. Pitzer, A. J. Stone, P. R. Taylor, and R. Lindh.
[18] P. J. Knowles, C. Hampel, and H.-J. Werner, J. Chem. Phys. **99**, 5219 (1993).
[19] A. Nicklass, M. Dolg, H. Stoll, and H. Preuss, J. Chem. Phys. **102**, 8942 (1995).
[20] F basis: T. H. Dunning, Jr., J. Chem. Phys. **90**, 1007 (1989); R. A. Kendall, T. H. Dunning, Jr., and R. J. Harrison, *ibid.* **96**, 6769 (1992); Cl basis: D. E. Woon and T. H. Dunning, Jr., *ibid.* **98**, 1358 (1993).

[21] A. Schäfer, C. Huber, and R. Ahlrichs, J. Chem. Phys. **100**, 5829 (1994).

[22] A. Bergner, M. Dolg, W. Kuechle, H. Stoll, and H. Preuss, Mol. Phys. **80**, 1431 (1993).

[23] M. Dolg, M. Diefenbach (personal communication).

[24] E. C. Moore, Atomic Energy Levels NBS Monogr. **467**, 1 (1949); **467**, 2 (1952); **467**, 3 (1958).

[25] R. J. Gdanitz and R. Ahlrichs, Chem. Phys. Lett. **143**, 413 (1988); R. J. Cave and E. R. Davidson, J. Chem. Phys. **89**, 6708 (1988); P. G. Szalay and R. J. Bartlett, Chem. Phys. Lett. **214**, 481 (1993). For the application in MOLPRO, see: H.-J. Werner and P. J. Knowles, Theor. Chim. Acta **78**, 175 (1990).

[26] For a discussion of the treatment of core electrons in correlated calculations, see, e.g., D. E. Woon and T. H. Dunning, Jr., J. Chem. Phys. **103**, 4572 (1995).

[27] S. Koseki, M. W. Schmidt, and M. S. Gordon, J. Phys. Chem. **96**, 10768 (1992); S. Koseki, M. S. Gordon, M. W. Schmidt, and N. Matsunaga, *ibid.* **99**, 12764 (1995).

[28] M. W. Schmidt *et al.*, J. Comput. Chem. **14**, 1347 (1993). The version for PC was compiled by A. A. Granovsky, Moscow State University.

[29] W. J. Stevens, M. Krauss, H. Basch, and P. G. Jasien, Can. J. Chem. **70**, 612 (1992).

[30] Because there is only a shallow minimum, one might question the appropriateness of these FOCl wave functions with fairly small basis sets for calculating the spin–orbit coupling constants. Actually, the qualitative nature of the wave function (e.g., positive Mulliken charge on Xe) is well reproduced even at this moderate level of theory, and the relative energies of the different states should also be acceptably well described. Some test calculations were performed, with the aim of probing the sensitivity of the spin–orbit coupling constants and of the SO corrections to the ground state energy to the level of theory. Thus, the basis set was changed, the CAS space was enlarged, the level of CI treatment was changed from only single excitations to no excitations (CAS wave functions only) or to single and double excitations (SOCI wave functions). All of these tests showed only small differences from the present results, which suggests that the FOCI wave functions used here are appropriate, at least within the approximate one-electron operator formalism applied.

[31] MOLCAS version 3: K. Andersson, M. R. A. Blomberg, M. P. Fülscher, V. Kellö, R. Lindh, P.-Å. Malmqvist, J. Noga, J. Olsen, B. O. Roos, A. J. Sadlej, P. E. M. Siegbahn, M. Urban, and P. O. Widmark, University of Lund, Sweden, 1994.

[32] NBO Version 3.1: E. D. Glendeningn, A. E. Reed, J. E. Carpenter, and F. Weinhold.

[33] GAUSSIAN 94, Revision E.l, M. J. Frisch, G. W. Trucks, H. B. Schlegel, P. M. W. Gill, B. G. Johnson, M. A. Robb, J. R. Cheeseman, T. Keith, G. A. Petersson, J. A. Montgomery, K. Raghavachari, M. A. Al-Laham, V. G. Zakrzewski, J. V. Ortiz, J. B. Foresman, J. Cioslowski, B. B. Stefanov, A. Nanayakkara, M. Challacombe, C. Y. Peng, P. Y. Ayala, W. Chen, M. W. Wong, J. L. Andres, E. S. Replogle, R. Gomperts, R. L. Martin, D. J. Fox, J. S. Binkley, D. J. Defrees, J. Baker, J. P. Stewart, M. Head-Gordon, C. Gonzalez, and J. A. Pople, Gaussian, Inc., Pittsburgh, PA, 1995.

[34] J. Holmes, Mass Spectrom. Rev. **8**, 513 (1989).

[35] T. T. Yang, J. A. Blauer, C. E. Turner, Jr., and G. A. Merry, Appl. Opt. **26**, 2533 (1987); D. H. Burde, T. T. Yang, D. G. Harris, L. A. Pugh, J. H. Tillotson, C. E. Turner, Jr., and G. A. Merry, *ibid.* **26**, 2539 (1987).

[36] S. G. Lias, J. E. Bartmess, J. F. Liebman, J. L. Holmes, R. D. Levin, and W. G. Mallard, J. Phys. Chem. Ref. Data **17**, 1 (1988).

[37] D. Schröder, N. Goldberg, W. Zummack, H. Schwarz, J. C. Poutsma, and R. R. Squires, Int. J. Mass Spectrom. Ion Processes **165/166**, 71 (1997); G. Hornung, C. A Schalley, M. Dieterle, D. Schröder, and H. Schwarz, Chem. Eur. J. **3**, 1866 (1997); C. A. Schalley, G. Hornung, D. Schröder, and H. Schwarz, Int. J. Mass Spectrom. Ion Processes **172/173**, 181 (1998); Chem. Soc. Rev. **27**, 91 (1998).

[38] P. J. MacDougall, G. J. Schrobilgen, and R. F. W. Bader, Inorg. Chem. **28**, 763 (1989).

[39] This interpretation is supported by the observation of a non-negligible (~ 0.06) norm of the τ_1 excitation vector in the coupled-cluster expansion around the minimum. We note that for all the other species studied here, the τ_1 vector was always of negligible magnitude (0.02 or smaller).

[40] J. Tellinghuisen, A. K. Hays, and G. C. Tilsone, J. Chem. Phys. **65**, 4473 (1976).

[41] See also: V. Aquilanti, D. Cappelletti, and F. Pirani, Chem. Phys. Lett. **271**, 216 (1997).

[42] For neutral NeH• as a similar example, see S. F. Selgren, D. E. Hipp, and G. I. Gellene, J. Chem. Phys. **88**, 3116 (1988).